Published in final edited form as:
Microsc Res Tech. 2011 March ; 74(3): 219–224. doi:10.1002/jemt.20896.

Denaturing of Single Electrospun Fibrinogen Fibers Studied by Deep Ultraviolet Fluorescence Microscopy

JEONGYONG KIM[1,*], **HUGEUN SONG**[1], **INHO PARK**[1], **CHRISTINE R. CARLISLE**[2], **KEITH BONIN**[2], and **MARTIN GUTHOLD**[2]

[1] Department of Physics, University of Incheon, Incheon 406-772, South Korea

[2] Department of Physics, Wake Forest University, Winston-Salem, North Carolina 27109

Abstract

Deep ultraviolet (DUV) microscopy is a fluorescence microscopy technique to image unlabeled proteins via the native fluorescence of some of their amino acids. We constructed a DUV fluorescence microscope, capable of 280 nm wavelength excitation by modifying an inverted optical microscope. Moreover, we integrated a nanomanipulator-controlled micropipette into this instrument for precise delivery of picoliter amounts of fluid to selected regions of the sample. In proof-of-principle experiments, we used this instrument to study, in situ, the effect of a denaturing agent on the autofluorescence intensity of single, unlabeled, electrospun fibrinogen nanofibers. Autofluorescence emission from the nanofibers was excited at 280 nm and detected at ~350 nm. A denaturant solution was discretely applied to small, select sections of the nanofibers and a clear local reduction in autofluorescence intensity was observed. This reduction is attributed to the dissolution of the fibers and the unfolding of proteins in the fibers.

Keywords

deep ultraviolet fluorescence microscopy; micropipette; fibrinogen; electrospinning; picoliter dispensation

INTRODUCTION

Fibrinogen, one of the most abundant proteins in blood plasma, has a molecular weight of about 340,000 g/mol and is composed of a pair of three polypeptide chains: two Aα-, two Bβ-, and two γ-chains. Fibrinogen is 45 nm long, it has a diameter of 4.5 nm and is shaped like a double dumbbell; its two globular end domains and a globular central domain are connected by 17 nm long coiled coils consisting of three alpha helices (Kollman et al., 2009). During blood coagulation thrombin removes four fibrinopeptides from fibrinogen, thus converting it to fibrin. Fibrin spontaneously aggregates in a half-staggered manner to form fibrin protofibrils. These protofibrils then aggregate laterally into larger fibers that branch to form a three-dimensional network that provides mechanical strength and stability to blood clots.

In addition to forming natural fibrin fibers, fibrinogen can also be spun into nanoscopic fibers via a process termed electrospinning (Carlisle et al., 2009; Wnek et al., 2003). To produce these electrospun fibers, a protein solution is extruded from a syringe and subjected to a high electric field between the syringe needle and a collecting plate (Reneker and Chun,

[*]Correspondence to: Jeongyong Kim, Department of Physics, University of Incheon, Incheon 406-772, South Korea. jeongyong@incheon.ac.kr.

1996). The electric field stretches and thins the fibers. Depending on spinning conditions, fibers with a diameter from 10 nm to 10 μm can be produced routinely. This range of diameters mimics the range of diameters formed by natural fibrin fibers and that of fibers in the extracellular matrix. Because of the nonimmunogenic nature of fibrinogen, and fibrinogen's natural role in wound healing (as outlined in the paragraph above), electrospun fibrinogen fibers are great candidates for tissue engineering applications (McManus et al., 2007a,b). Carlisle et al. (2009) has recently determined the detailed mechanical properties of electrospun fibrinogen fibers, in an effort to determine the properties of nonimmunogenic nanofibers that are suitable for tissue engineering and other biomedical applications. Visualization in these and many other experiments usually requires fluorescent labeling of the protein, which may alter function or interfere with applications, in which the addition of organic fluorescent molecules may not be feasible or desirable. A solution to this problem is visualization via the native autofluorescence of many proteins, including fibrinogen.

Each fibrinogen monomer contains 72 tryptophan residues ($\alpha = 11$; $\beta = 14$; $\gamma = 11)_2$, 104 tyrosine residues ($\alpha = 9$; $\beta = 21$; $\gamma = 22)_2$, and 108 phenylalanine residues ($\alpha = 20$; $\beta = 12$; $\gamma = 22)_2$ (http://www.ncbi.nlm.nih.gov/sites/entrez). Fluorescence is usually dominated by tryptophan residues since the fluorescence intensity of tryptophan is about eight times larger than that of tyrosine and 140 times larger than that of phenylalanine. The absorbance maximum for tryptophan and tyrosine is near 280 nm, whereas the less important phenylalanine absorbs at around 260 nm. This is also true for fibrinogen as the absorbance maximum is at 280 nm and the emission maximum is at 350 nm (Gonçalves et al., 2006, 2007). Most tryptophan residues are situated inside the hydrophobic core of the protein. When the protein undergoes a conformation change that exposes some of the tryptophan residues to the surrounding polar solvent, the fluorescence quantum yield of the exposed tryptophan is usually significantly reduced (Vivian and Callis, 2001). Therefore, tryptophan fluorescence has been used to diagnose the structural and conformational change of proteins (Gensch et al., 2004). Gonçalves et al. (2007) observed the reduction of tryptophan fluorescence in fibrinogen while it engaged in a ligand interaction with β-estradiol, which functions to decrease the risk of diseases due to fibrinogen aggregation. Their study showed that the β-estradiol binding process induces a conformational change in fibrinogen; and the structural denaturing of fibrinogen caused a reduction of tryptophan fluorescence. The research of Gonçalves et al. (2006, 2007), Vivian and Callis (2001), and Gensch et al. (2004) support tryptophan fluorescence as a good method for monitoring conformational change in fibrinogen molecules.

Fibrinogen fibers formed by electrospinning may have useful medical and other applications; they are easy to make, they are durable, and they have intrinsic tryptophan fluorescence, making them a good choice to test deep ultraviolet (DUV) fluorescence microscopy with an integrated micropipette for dispensing chemical agents. The tryptophan fluorescence from electrospun fibrinogen fibers is used to gain information on the protein structure within these single nanofibers.

To be able to monitor tryptophan fluorescence characteristics of single fibrinogen fibers, such as emission intensity and emission wavelength, photoexcitation needs to be in the 200–300 nm wavelength range. UV microscopy has unique advantages over visible light microscopy, one being that biological samples have strong absorption and intrinsic fluorescence in the UV wavelength range. This feature of UV microscopy has been used in various applications, such as quantitative mapping of nucleic acid and protein mass in live-cells (Zeskind et al., 2007), distinguishing and identifying protein crystals (Judge et al., 2005), investigating the dynamic behavior of the plasma membrane (Lang-Pauluzzi, 2000) and differentiating cancer cells from healthy cells (Palmer et al., 2003). UV microscopy with an integrated picoliter micropipette dispenser has not yet been described in the literature.

In this study, we constructed a DUV microscope on an inverted optical microscope equipped with a three-axis nanomanipulator. The nanomanipulator provided 40-nm accuracy positioning of the micropipette, while the sample could be viewed via DUV. This unique arrangement enabled us to obtain DUV fluorescence images of unlabeled, electrospun fibrinogen nanofibers while they were chemically modified at select, micrometer-sized regions. Dispensing picoliter quantities of chemical denaturant caused a reduction in the fluorescence of the electrospun fibrinogen fibers, which we attribute to disintegration of the fiber and denaturing of the protein.

MATERIALS AND METHODS

DUV Microscope Set Up

Figure 1 shows the schematic set-up of our DUV microscope and the nanomanipulator (Sutter Instruments, MP-285 Motorized Micromanipulator with Rotary Optical Device) developed around an inverted optical microscope (Zeiss Axiovert 200, Zeiss, NY). Some upright UV microscopes are commercially available. However, an inverted microscope is required if simultaneous nanomanipulation or atomic force microscope (AFM) measurements are done while UV fluorescence images are collected. Thus, we modified an existing inverted optical microscope into a DUV fluorescence microscope. An epifluorescence configuration was used and a UV LED (Sensor Technology, UVTOP280) that emits 280 nm wavelength light was used as the fluorescence excitation source. To efficiently collect the LED light, we used a fused silica lens (focal length = 30 mm) in front of the LED and focused the LED light onto the back aperture of the objective for efficient coupling of UV light to the objective.

A UV transmitting objective (1.25 NA, 40×, Partec Instruments) was used to focus the excitation UV light onto the sample and to collect the emitted fluorescence from the sample. The original filter box of the microscope under the objective lens was replaced with a lab-made filter box containing a dichroic mirror (Semrock, FF310-Di01) and a bandpass emission filter (Semrock FF01-357/44 nm). The tube lens and the port selecting optics originally installed inside the microscope, which have low transmission efficiency at wavelengths below 400 nm, were bypassed using a 45° reflecting mirror. A UV silica lens (focal length = 150 mm) was used as a tube lens to form an image on a CCD camera (Hamamatsu EM-CCD C9100). Although not intended for deep-UV imaging, this low-light-detection CCD camera has a quantum efficiency of 0.4 at 400 nm wavelength, and showed a reasonable sensitivity (estimated 0.25 quantum efficiency) to the fluorescence at ~350 nm wavelength. The tryptophan fluorescence imaging capabilities were tested by obtaining a fluorescence image of pristine tryptophan (Sigma Adrich) dried from 1 M aqueous solution on a quartz cover slip (Fig. 1).

Sample Preparation

Fibrinogen fibers were prepared by electrospinning (Carlisle et al., 2009; Reneker and Chun, 1996; Wnek et al., 2003). The fibrinogen spinning solution consisted of one part 10× minimal essential medium (MEM, Gibco, Invitrogen Cell Culture), nine parts 1,1,1,3,3,3-hexafluoro-2-propanol (HFP; Sigma-Aldrich Chemical), and 100 mg/mL bovine fibrinogen (final concentration, Sigma-Aldrich Chemical Co). HFP is a volatile, organic solvent commonly used in electrospinning. Because of its volatility, HFP evaporates during electrospinning resulting in dry protein nanofibers. Like many proteins, fibrinogen is stable and soluble in HFP; fibrinogen does not denature in this solvent, though it does become somewhat more α-helical (Carlisle et al., 2009).

The total volume of solution transferred to the syringe was 1.5 mL. A 20-gauge syringe (blunt tip) was placed into the syringe pump and aimed horizontally at the cleaned quartz substrate attached to a metal acceptor plate placed at a distance of 20 cm. The syringe pump rate was set to 4 mL/h. A voltage of 20 kV was applied to the metal tip of the syringe containing the fibrinogen solution. We simultaneously started the syringe pump and the voltage. Typical deposition time was 30 s. The typical diameter of the single fibers was measured to be ~30 nm, as determined from AFM imaging.

UV Fluorescence Spectra

Fluorescent spectra of the spinning solution were taken using a LS 55 Fluorescence Spectrometer (Perkin Elmer). The excitation wavelength was set to 280 nm to match the wavelength of the excitation LED photodiode and the spectra were collected for wavelengths between 300 and 600 nm. Four samples were tested for fluorescence; HFP, HFP plus MEM, fibrinogen in HFP, and fibrinogen in HFP plus MEM. The solutions were prepared so that the MEM and fibrinogen concentrations were both 30× more dilute than the spinning solution. Figure 2 shows the fluorescence spectra. HFP and HFP plus MEM show little fluorescence at 357 nm, while fibrinogen in HFP and fibrinogen and HFP plus MEM show significant fluorescence.

Procedure for the Selective Denaturing and Picoliter Liquid Dispensing

We used a phosphate buffer solution (PBS) of guani-dine hydrochloride (Gdn-HCL) at concentrations of 0.1, 0.5, 1, 2, and 3 M, to denature the fibrinogen fibers. To apply denaturant to the selected target area, we used a prepulled glass nanopipette (WPI) attached to a three-axis nanomanipulator (Sutter P285). A prepulled glass pipette, with an aperture size of 400 nm, was attached to a PVC tube and a syringe. The syringe allowed the denaturant to be applied to and removed from the sample by manually applying positive and negative pressure to the syringe piston. With this setup we were able to control the size of the denaturant drop on the sample surface. The movement of the pipette and denaturant application process were monitored throughout the length of the experiment with the inverted microscope.

RESULTS

We took fluorescence spectra to test the native fluorescence of fibrinogen and the buffers. As can be seen in Figure 2, fibrinogen shows strong fluorescence in HFP and HFP plus MEM, whereas the HFP and HFP plus MEM alone show no significant fluorescence at 357 nm, the wavelength of the bandpass filter of our UV microscope. The majority of the native fibrinogen fluorescence is most likely due to the 72 tryptophan residues which are situated inside the hydrophobic core of the protein. Exposure to polar solvents causes a drastic reduction in the fluorescence quantum yield of tryptophan (Gensch et al., 2004; Gonçalves et al., 2007; Vivian and Callis, 2001).

Figure 3 shows a set of bright-field transmission and UV fluorescence images of fibrinogen fibers, obtained by our DUV microscope. A DUV fluorescence image (Fig. 3a) is taken before the application of about 30 pL of 3 M denaturant solution. Figure 3b shows a bright-field microscope image with the 30 pL-sized drop of denaturant sitting on fibrinogen nanofibers, and Figure 3c, once again a DUV image, is taken ~1 min after the denaturant application. The UV light exposure time for taking a fluorescence image was 5 s. The viewing areas of these three images are exactly the same. By comparing Figures 3a and 3c, we notice that the intensity of the fluorescence signal from the part of the fibrinogen fibers directly immersed in the denaturant (indicated with an arrow) is most affected. The fluorescence signal in this area was so weak that it was difficult to see the fibrinogen fibers

in Figure 3c. The part of the fibrinogen fibers that were not immersed but soaked with the denaturant solution, either at the edge of the drop or from wicking, also emitted a considerably reduced fluorescence signal while the other fibrinogen fibers not in contact with the denaturant do not show any apparent reduction in fluorescence.

For a quantitative analysis of the fluorescence intensity change, the "y-average[*]" of the fluorescence distribution was determined within the rectangular area indicated in Figures 3a and 3c. The fibrinogen fiber in the rectangular area in Figure 3 was not fully immersed but apparently some part of the denaturant solution was wicked along the fiber reducing the fluorescence in that area. The result of the y-averaging on this area obtained from Figures 3a and 3c is shown in Figure 3d. The integrated area of the y-averaged profile above the background was measured to represent the fluorescence intensity of the fibrinogen fiber in the selected rectangular area. With this scheme, we found the fluorescence intensity of the rectangular area was reduced by 65% after the denaturant application. This confirms that exposure to the denaturant caused a reduction of tryptophan fluorescence of electrospun fibrinogen fibers.

We carried out a total of 15 sets of similar experiments with six varying concentrations of denaturant which were 0, 0.1, 0.5, 1, 2, and 3 M and obtained the same number of image sets. 0 M represents PBS buffer solution without denaturant. Each image set consists of two fluorescence images of the same viewing area obtained before and after the denaturant application. For the quantitative comparison, three different rectangular areas were selected in all fluorescence images depending on proximity to the dispensed denaturant solution; an *intact area* represents a part of the fiber that has no direct or indirect contact with the denaturant solution, an *immersed part* is the part of the fiber directly under the dispensed denaturant, and a *soaked part* is the part of the fiber adjacent to the immersed area and soaked by wicking. Figure 4, which summarizes the analysis of these results, shows the amount of the change in the fluorescence intensity due to the denaturant application, versus denaturant concentration values.

The statistical results in Figure 4 do not suggest that higher molar concentrations induced a greater reduction in fluorescence; however, it appears that the immersed part and the soaked part emitted considerably less fluorescence signal than the intact part in all concentration experiments except the 0 M case. We notice that the intact area and the 0 M case also show some reduction in fluorescence even though there was no contact with denaturant in that area. This reduction in fluorescence, not related to the denaturant is most likely due to UV photooxidation, which is discussed in the following section.

DISCUSSION

We used DUV imaging to observe a fluorescence reduction in electrospun fibrinogen nanofibers as picoliter amounts of denaturing solution were applied to the fibers. To obtain the fluorescence of tryptophan, the fibrinogen fibers were exposed to UV irradiation for 5 s for each image. A natural reduction of fluorescence due to UV exposure, called photooxidation (Aseichev et al., 2002), must be considered when discussing fluorescence reduction due to protein denaturing. In our results comparing the fluorescence images before and after the denaturant application, we observed a decrease of fluorescence in intact fibrinogen fibers, which may only be explained by UV photooxidation.

[*]The profiles of the horizontal (*x*) lines comprising the selected rectangle are all summed through the vertical (*y*) axis and averaged to give a single cross-sectional profile.

Because we selectively denatured the fibrinogen fibers by applying the denaturant only to a limited area of the viewing field of our DUV microscope, we were able to differentiate the fluorescence intensity reduction caused by photooxidation from that caused by the denaturant. As seen in Figure 4, the fluorescence reduction observed in electrospun fibrinogen fibers exposed to the denaturant was more severe than what was observed in intact areas, and therefore we believe the denaturant is responsible for most of the observed fluorescence reduction of the fibers.

The reason for the reduced fluorescence of fibrinogen fibers caused by denaturant is most likely twofold: conformational change of protein structures in fibrinogen fibers induced by the denaturant, which in turn reduced the tryptophan fluorescence, and the physical dissolving of fibrinogen fibers into the denaturant solution. We observed that some of the fibers exposed to the denaturing solution became thicker, as if swelling. This swelling of the fibrinogen fibers was mostly observed at higher concentrations of the denaturant but was not observed when buffer solution or water was applied in the same manner. This indicates that the denaturant induced a physical change in the fibrinogen fibers, and therefore, there may be some dissolution of the fibers due to the denaturant.

We obtained a number of images of fibrinogen fibers selectively exposed to denaturing solutions of varying concentrations from 0.1 to 3 M and the result of a quantitative analysis of these images is displayed in Figure 4. The immersed parts and the soaked parts of the fibrinogen fiber in all concentrations other than 0 M showed a clear reduction of fluorescent intensity, while the intact part showed a minimal reduction which is due to the UV oxidation as discussed above. We note that there is a larger reduction in fluorescence intensity in immersed parts than soaked parts, which is expected because immersed parts are more severely and extensively influenced by the denaturant solution than the soaked parts.

However, higher concentrations of denaturant did not necessarily result in a larger reduction of fluorescence, and we do not see any clear correlation between denaturant molar concentration and the degree of fluorescence reduction observed. A previous study on denaturing fibrinogen using Gdn-HCL reported that Gdn-HCL caused a reduction of fluorescence in fibrinogen only at concentrations above 2 M and that no noticeable change in fluorescent intensity was observed at concentrations of 1 M or less of Gdn-HCL (Gonçalves et al., 2006). In our experiment using Gdn-HCL to denature individual electrospun fibrinogen fibers, we did not observe such a threshold behavior. Furthermore, concentrations as low as 0.1 M of Gdn-HCL seemed to be sufficient to cause considerable reduction in the fluorescence of fibrinogen fibers. This could be due to the interaction of HFP with fibrinogen in the electrospinning process, since HFP has been shown to change the alpha helical propensity of fibrinogen molecules (Carlisle et al., 2009), therefore making the fibrinogen molecule in the fiber different from the oligomers previously studied. On the other hand, it could be because we used pulled glasspipettes with a submicron size hole to apply denaturant solution, and drying of buffer at the glass pipette aperture may have increased the molar concentration of denaturant above the originally intended concentration.

SUMMARY

We successfully developed a DUV microscope and obtained tryptophan fluorescence images of unlabeled electrospun fibrinogen fibers. Using the DUV microscope and a nanomanipulator, we locally denatured electrospun fibrinogen fibers by applying a Gdn-HCL solution and observed a significant reduction in the tryptophan fluorescence of the fibrinogen fibers. The observed reduction of tryptophan fluorescence was attributed partly to the conformational change of protein structures in the fibrinogen fibers. We showed that

DUV microscopy can be used as a powerful tool for in situ studying of structural changes in fibrinogen molecules in electrospun fibrinogen fibers.

Acknowledgments

Contract grant sponsor: National Research Foundation of Korea (NRF); Contract grant numbers: 2007-02939, 2008-83859, 2009-89501; Contract grant sponsor: National Science Foundation (NSF); Contract grant number: CMMI-0646627; Contract grant sponsor: American Heart Association; Contract grant number: 081503E.

References

Aseichev AV, Azizova OA, Zhambalova BA. Effect of UV-modified fibrinogen on platelet aggregation in platelet-rich plasma. Bull Exp Biol Med. 2002; 1:41–43. [PubMed: 12170303]

Carlisle CR, Coulais C, Namboothiry M, Carroll DL, Hantgan RR, Guthold M. The mechanical properties of individual, electrospun fibrinogen fibers. Biomaterials. 2009; 30:1205–1213. [PubMed: 19058845]

Gensch T, Hendriks J, Hellingwerf KJ. Tryptophan fluorescence monitors structural changes accompanying signalling state formation in the photocycle of photoactive yellow protein. Photochem Photobiol Sci. 2004; 3:531–536. [PubMed: 15170481]

Gonçalves S, Santos NC, Martins-Silva J, Saldanha C. Fibrinogen-beta-estradiol binding studied by fluorescence spectroscopy: Denaturation and pH effects. J Fluores. 2006; 16:207–213.

Gonçalves S, Santos NC, Martins-Silva J, Saldanha C. Fluorescence spectroscopy evaluation of fibrinogen-beta-estradiol binding. J Photochem Photobiol B: Biol. 2007; 86:170–176.

Judge RA, Swift K, Âlez CG. An ultraviolet fluorescence-based method for identifying and distinguishing protein crystals. Acta Crystallogr Sect D: Biol Crystallogr. 2005; 61:60–66. [PubMed: 15608376]

Kollman JM, Pandi L, Sawaya MR, Riley M, Doolittle RF. Crystal structure of human fibrinogen. Biochemistry. 2009; 48:3877–3886. [PubMed: 19296670]

Lang-Pauluzzi I. The behaviour of the plasma membrane during plasmolysis: A study by UV microscopy. J Microsc Oxford. 2000; 198:188–198. [PubMed: 10849197]

McManus M, Boland E, Sell S, Bowen W, Koo H, Simpson D, Bowlin G. Electrospun nanofibre fibrinogen for urinary tract tissue reconstruction. Biomed Mater. 2007a; 2:257–262. [PubMed: 18458483]

McManus MC, Boland ED, Simpson DG, Barnes CP, Bowlin GL. Electrospun fibrinogen: Feasibility as a tissue engineering scaffold in a rat cell culture model. J Biomed Mater Res Part A. 2007b; 81:299–309.

Palmer GM, Keely PJ, Breslin TM, Ramanujam N. Autofluorescence spectroscopy of normal and malignant human breast cell lines. Photochem Photobiol. 2003; 78:462–469. [PubMed: 14653577]

Reneker DH, Chun I. Nanometre diameter fibres of polymer, produced by electrospinning. Nanotechnology. 1996; 7:216–223.

Vivian JT, Callis PR. Mechanisms of tryptophan fluorescence shifts in proteins. Biophys J. 2001; 80:2093–2109. [PubMed: 11325713]

Wnek GE, Carr ME, Simpson DG, Bowlin GL. Electrospinning of nanofiber fibrinogen structures. Nano Lett. 2003; 3:213–216.

Zeskind BJ, Jordan CD, Timp W, Trapani L, Waller G, Horodincu V, Ehrlich DJ, Matsudaira P. Nucleic acid and protein mass mapping by live-cell deep-ultraviolet microscopy. Nature Methods. 2007; 4:567–569. [PubMed: 17546037]

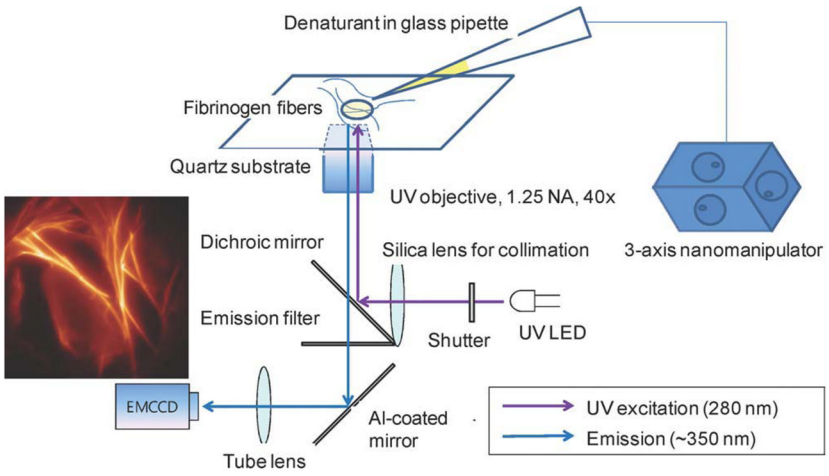

Fig. 1.

Schematic of the DUV microscope developed for imaging tryptophan fluorescence of fibrinogen fibers. A three-axis nanomanipulator was used to maneuver the pipette to selectively apply a denaturant solution to the electrospun fibrinogen fibers prepared on the quartz substrate. [Color figure can be viewed in the online issue, which is available at www.interscience.wiley.com.]

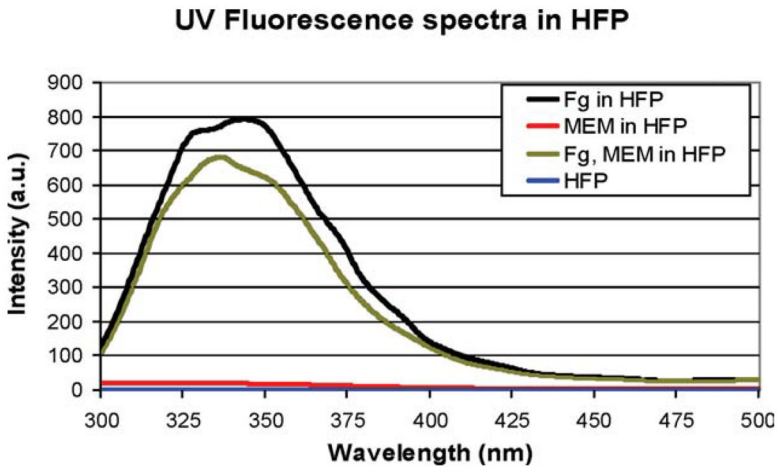

Fig. 2.

Fluorescence spectra of the spinning solution and its components. HFP (blue) and MEM (red) do not fluoresce significantly at 357 nm, the wavelength of the bandpass emission filter. However, a fluorescence peak at 357 nm is seen due to fibrinogen (Fg) in HFP (black) and in HFP plus MEM (gold). [Color figure can be viewed in the online issue, which is available at www.interscience.wiley.com.]

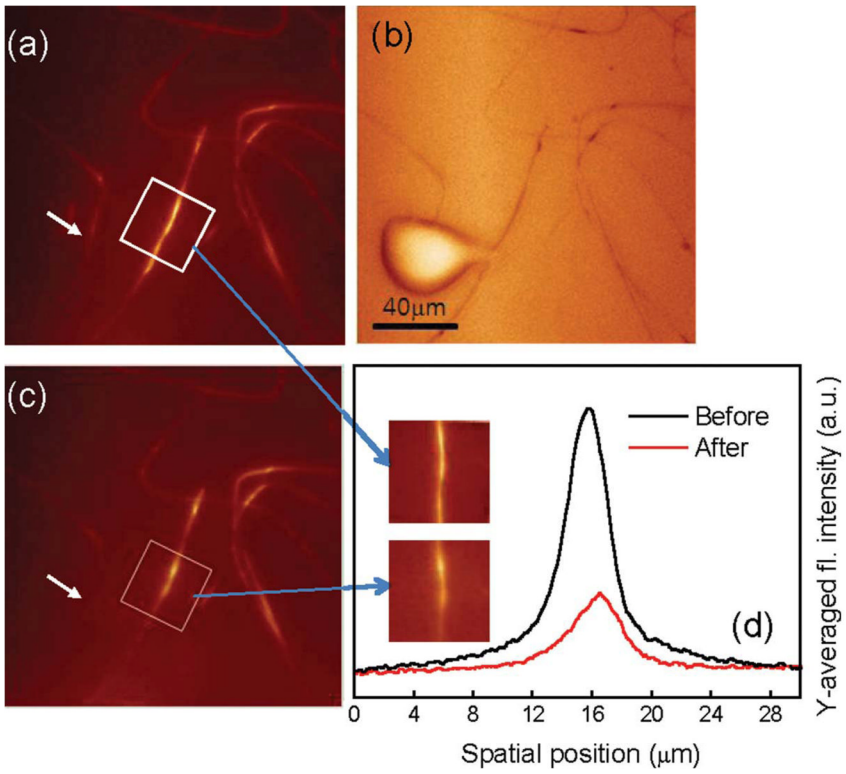

Fig. 3.

(**a**, **c**) The UV fluorescence images taken before and after the application of about 30 pL of 3 M denaturant solution, respectively. The bright-field image in (**b**) shows the drop of denaturant applied to the fibrinogen fibers. (a–c) are the same fields of view and were taken in alphabetical order. The rectangle in (c) represents the area selected for fluorescence y-averaging to compare the intensity of the fibrinogen fibers before and after denaturing. The results of the y-averaging are displayed in (**d**) and show a 65% reduction in fluorescence due to the denaturant. Insets in (d) are cropped images from the fluorescence images obtained before (above) and after (below) the denaturant application. [Color figure can be viewed in the online issue, which is available at www.interscience.wiley.com.]

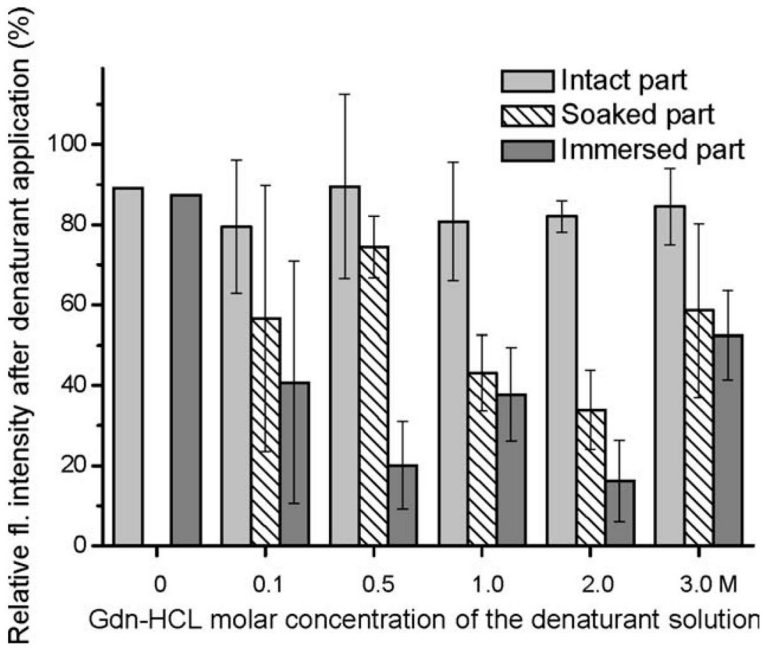

Fig. 4.

Fluorescence intensities relative to the initial values obtained before denaturant application versus Gdn-HCL molar concentration of denaturant solution. Three rectangular areas of the immersed part, soaked part, and intact part were selected from each fluorescence image obtained before and after the denaturant application and the ratio between the average fluorescence intensities before and after the denaturant application were calculated. The error bars represent the standard deviations of the mean values obtained from plural sets of images for each concentration. A total of 15 image sets were used for the analysis.